Effect of bonding and antibonding character of electronic states on their tunneling spectra

Omar Lahrache, Mehdi Bouatou, Cyril Chacon, Yann Girard, Yannick Dappe, Jérôme Lagoute, Alexander Smogunov

Effect of bonding and antibonding character of electronic states on their tunneling spectra

Omar Lahrache,[1] Mehdi Bouatou,[2] Cyril Chacon,[2] Yann Girard,[2] Yannick J. Dappe,[1]
Jérôme Lagoute,[2] and Alexander Smogunov[1]
[1]*SPEC, CEA, CNRS, Université Paris-Saclay, CEA Saclay, Gif-sur-Yvette F-91191, France*
[2]*Université de Paris, CNRS, Laboratoire Matériaux et Phénomènes Quantiques, 75013 Paris, France*

(Received 3 January 2022; accepted 17 March 2022; published 30 March 2022)

We argue that the bonding or antibonding character of electronic states of a substrate can influence significantly the observed scanning tunneling microscopy (STM) spectra. In particular, the antibonding states formed by nonorthogonal orbitals of the substrate present much stronger extension in the vacuum compared to corresponding bonding combinations and are therefore much more visible in STM experiments. A clear example is provided by black phosphorus (BP), which is one of the most interesting two-dimensional layered materials nowadays. The pronounced asymmetry in its conductance spectra, with significant increase at positive voltage, can be attributed to the antibonding nature of the conduction band compared to the bonding valence band, despite the same p_z-orbital character. Furthermore, this asymmetry can be at the origin of different broadenings of frontier molecular orbitals observed experimentally for molecules on BP.

DOI: 10.1103/PhysRevB.105.125420

I. INTRODUCTION

Scanning tunneling microscopy (STM) and related spectroscopy measurements (STS) are among the most powerful techniques in surface science, allowing us to characterize the local geometry of surfaces (pure or with various adsorbates or defects) as well as to probe their electronic states as a function of energy. The tunneling conductance, dI/dV, measured by STS can be generally related within the well-known Tersoff-Hamann approach to the local density of states (LDOS) of the substrate at the STM tip position (vacuum LDOS). Thus the tunneling conductance depends not only on the amount of electronic states but also on their extension outside the sample. The latter is determined by several factors, such as the main atomic character of electronic states—s, p or d—or their spatial orientation. In particular, s-, p_z- or d_{z^2}-originated states, oriented in the out-of-plane direction, usually dominate the STS spectra compared to other in-plane p or d states. The influence of these orbital symmetry effects on the obtained STM images has been widely discussed in literature, in connection to substrate orbitals [1–3] as well as to the orbital character of the STM tip states [4,5].

The extension of electronic wave functions in the vacuum can also depend on their organization inside the substrate—a point which, to the best of our knowledge, has not yet been discussed in literature in connection with STS measurements. We will demonstrate, in particular, that electronic states with bonding (B) character within the sample should in general be more compressed to the bulk and therefore spread much less outside than corresponding antibonding (AB) combinations. That should result in significant asymmetry of STS signals seen from B and AB states.

We illustrate the idea on a very representative example of black phosphorus (BP)—one of the two-dimensional (2D) layer-structured materials which has recently attracted a great deal of attention [6–8] due to possible superconductivity at low temperature, high carrier mobility at room temperature, or his semiconductor properties with a tunable band gap [9]. Recent STS studies of BP have reported a clear asymmetry in the differential conductance around the gap. It was argued [10] that a much larger contribution from the conduction band (CB) is due to its p_z-like character, while the valence band (VB) is provided by other orbitals (presumably, p_x or p_y) which are in-plane orbitals and therefore decay much faster in the vacuum. We will suggest in the following another argument: both the VB and CB mainly originate from p_z orbitals but have different character within the single P layer and as a consequence very different extensions in the vacuum. The VB is composed of bonding states (low extension), while the CB has antibonding character (high extension), which would explain the highly asymmetric STS curves showing a much more pronounced signal at positive voltage.

II. COMPUTATIONAL AND EXPERIMENTAL DETAILS

Density Functional Theory (DFT) calculations for BP were performed using the plane-wave electronic structure package QUANTUM ESPRESSO [11,12] within the Perdew-Burke-Ernzerhof parametrization for the exchange-correlation functional (PBE). The lattice parameters for a slab of BP were set to $a = 3.348$ Å, $b = 4.587$ Å and $c = 11.033$ Å along the X, Y, and Z directions, respectively, corresponding to those reported for bulk BP [10]. The unit cell of bulk BP therefore contains two P monolayers (four atoms per each one). The vacuum region of 20 Å was added to separate the slabs in the Z direction and to avoid their artificial interaction. Energy cutoffs of 30 and 300 Ry were used for the wave functions and the charge density, respectively. The two surface layers

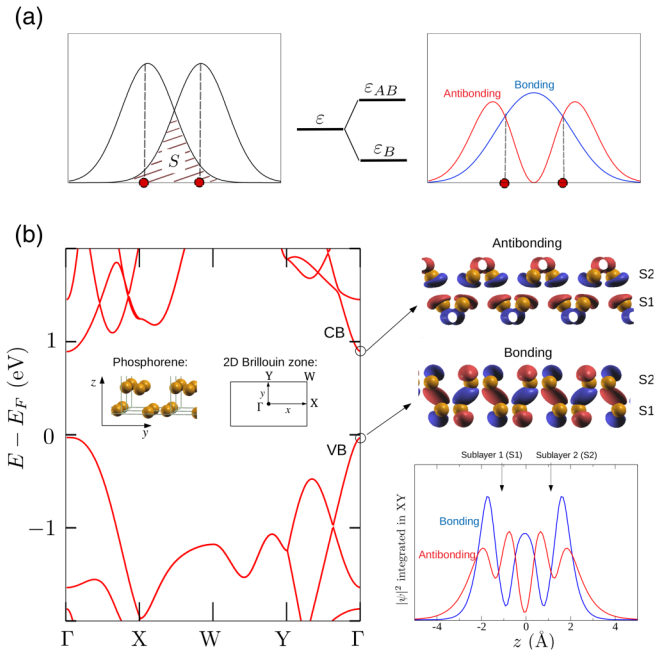

FIG. 1. Bonding and antibonding states from nonorthogonal orbitals: (a) Simple model with two Gaussians and overlap S. When hybridized they form the bonding and antibonding states with spatial distributions shown on the right panel. (b) Monolayer of BP: the band structure (left) and images of the B and AB states at the Γ point (right). Their XY plane integrated plots, presented below, clearly show a stronger spread in the vacuum for the AB state compared to the B one.

on both sides of the slab were allowed to relax while the other layers were kept at their bulk positions. The structural optimization proceeded until atomic forces became smaller than 10^{-4} Ry/bohr. Van der Waals interactions were taken into account using semiempirical Grimme's corrections as implemented in the QUANTUM EXPRESSO package. In the case of a BP monolayer, all atomic positions were relaxed. The self-consistent calculations were done with a $20\times20\times1$ k-point mesh, while the density of states (DOS) were calculated with a finer mesh of $80\times80\times1$ k points. STM measurements were performed using a low-temperature STM apparatus (Omicron) working at 4.6 K at a pressure lower than 1×10^{-10} mbar. The dI/dV spectra were acquired using a lock-in detector at a frequency of ca. 750 Hz and a modulation amplitude of 35 mV. The measurements were performed with an electrochemically etched tungsten tip. Before measuring on BP, the tip was calibrated on a Au(111) surface until it showed the Shockley surface-state feature in the spectroscopic measurements. The BP sample was purchased from the 2D Semiconductors company and cleaved under ultrahigh vacuum before measurement.

III. RESULTS AND DISCUSSION

A. Model and monolayer of BP

Quite generally, two degenerate orbitals under hybridization will split, forming bonding and antibonding (molecular) states as it is illustrated in Fig. 1(a). These two states have rather different shapes: while the B state shows a strong localization in between the two sites (making a bond), the AB state presents a node there and spreads much more on both sides in the vacuum region. These features can be readily reproduced by a simple model with two Gaussians simulating the two atomic wave functions with overlap S. The corresponding model Hamiltonian is parametrized with diagonal elements ε, and off-diagonal hopping integrals δ. The B/AB states are then found by solving the 2×2 eigenvalue problem, $H\psi = ES\psi$. The wave function distributions for the two states, $|\psi_B|^2$ and $|\psi_{AB}|^2$, clearly show the features discussed above, in particular, much stronger extension of the AB state compared to the B one. It is important to note the crucial role of the overlap S since for the orthogonal basis, $S = 0$, the B/AB states display identical spatial extensions in the vacuum.

We illustrate the above idea on a representative case of black phosphorus. We first consider a BP monolayer [Fig. 1(b)], which can be seen as composed of two sublayers. We will see that this specific feature of BP plays the role of the two sites discussed above. The band structure shows a gap of about 0.8 eV at the Γ point. The valence and conduction bands are composed of bonding and antibonding states between the two sublayers. This can be easily seen through direct visualization of electron wave functions at the Γ point, as shown on the right panels of Fig. 1(b). The plot of integrated (in the XY plane) values along the Z direction perpendicular to the BP layer reveals the clear similarity to the above model picture. In particular, the AB state spreads farther outside the layer than the B state. This point might be especially important for STS measurements where the vacuum DOS is essentially probed by the STM tip so that AB states are expected to be much more visible.

B. BP slab of ten layers

In order to simulate a BP surface, we consider a slab of ten P layers stacked in an *AB*... sequence along the Z direction. The B layer is shifted by half of a unit-cell period along the X axis with respect to the A layer which corresponds to the minimum energy configuration. Figure 2(a) shows the band structure of such a slab along the same k path as for the monolayer above. Compared to the monolayer, each band splits roughly into ten bands, in particular, the VB and CB bands encircled around the Γ point on the right. Because of this splitting, the gap, 0.3 eV, is noticeably decreased compared to the monolayer case. The p-orbital resolved DOS at the Γ point, presented in Fig. 2(b), shows that both VBs and CBs are dominated by p_z orbitals (with a small admixture of p_y character in the CBs), seen as the peaks in the p_z DOS. In order to discriminate between VBs and CBs and also prove their B and AB character (within each P monolayer), respectively, we plot on the lower panel of Fig. 2(b) the local DOS (LDOS) integrated within two different thin plates—one in the vacuum, at 4 Å above the surface, and another one inside the surface P layer as illustrated on the right of Fig. 2(b). One can now clearly see that the VBs strongly dominate the inside layer LDOS, while the CBs dominate the vacuum LDOS. This confirms the AB character of the CBs, with their strong extension into the vacuum and the B character of VBs states, in agreement with the monolayer case discussed above.

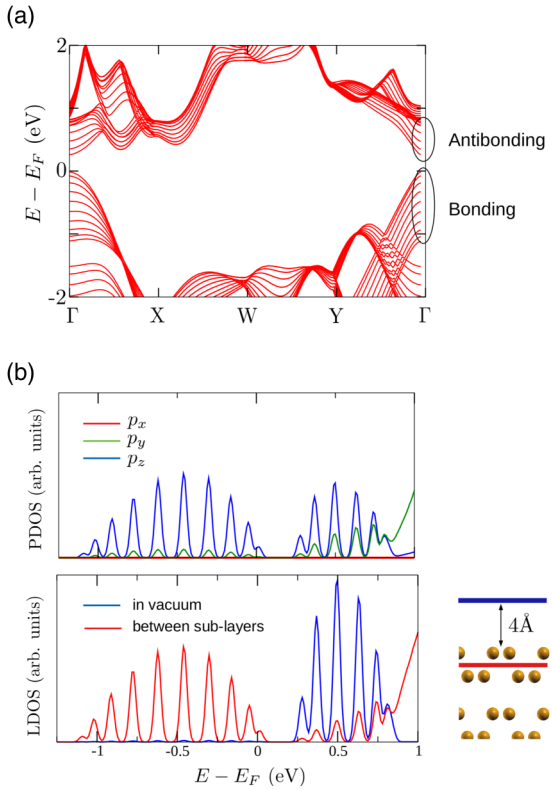

FIG. 2. BP slab of ten layers: (a) band structure; (b) upper panel: projected DOS (PDOS) on different p orbitals of the surface layer at the Γ k-point; lower panel: the local DOS (LDOS) at the Γ integrated over thin plates placed at different z positions shown on the right panel.

Finally, after a detailed analysis of the states at the Γ point, we present in Fig. 3(a) the total DOS integrated over the full 2D Brillouin zone. The main conclusions drawn from the Γ-point case remain unchanged. In particular, the p_z-DOS, which should be the most relevant for STM measurements due to its orbital orientation, displays again a rather symmetric shape to the right and to the left of the gap. On the contrary, the LDOS in the vacuum, Fig. 3(b), is clearly asymmetric, with a large increase at positive energies where AB states are present compared to negative energies dominated by B states. This asymmetry is a robust result and becomes even more pronounced with increasing the distance from the surface, from 4 to 6 Å, as shown in the figure. One can conclude, therefore, that the STM tip, probing the vacuum LDOS according to the well-known Tersoff-Hamann approach, should provide a rather asymmetric spectra with a strong enhancement at positive voltages, reflecting the strong asymmetry in spatial distributions between the B and AB states.

Experimentally, this asymmetry is observed as shown in Fig. 4. The dI/dV spectrum of bulk BP around the Fermi level exhibits a 0.3-V gap corresponding to the gap of bulk BP [7,13,14]. Outside the gap, the dI/dV signal exhibits a stronger increase in the conduction band than in the valence band [Fig. 4(a)]. At larger sample bias this asymmetry still holds, with a much larger signal at positive voltage than at negative voltage. This experimental spectrum compares very well with the calculated LDOS in Fig. 3, which confirms the theoretical description given above.

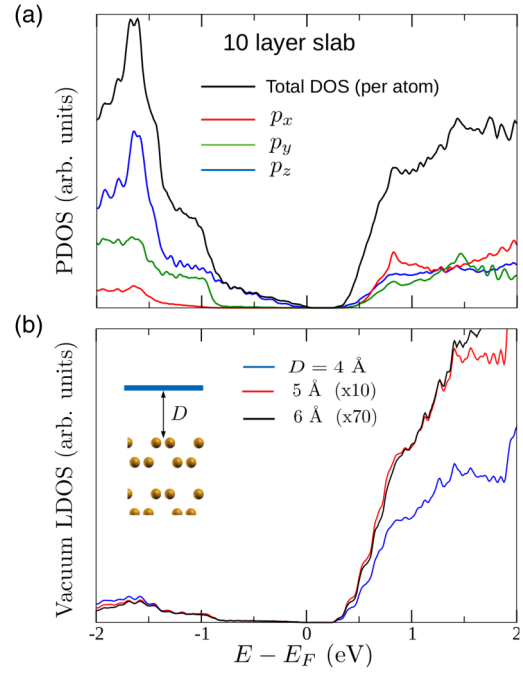

FIG. 3. DOS of ten-layer slab integrated over full 2D Brillouin zone: (a) total DOS and PDOS on different p orbitals of the surface layer and (b) LDOS in the vacuum plates at different heights D.

This asymmetry in the LDOS has an interesting consequence on the interaction of BP with adsorbates. Previous experiments have shown that molecular adsorbates on BP undergo an asymmetric broadening of the molecular states. For iron tetraphenylporphyrin on BP, the lowest unoccupied

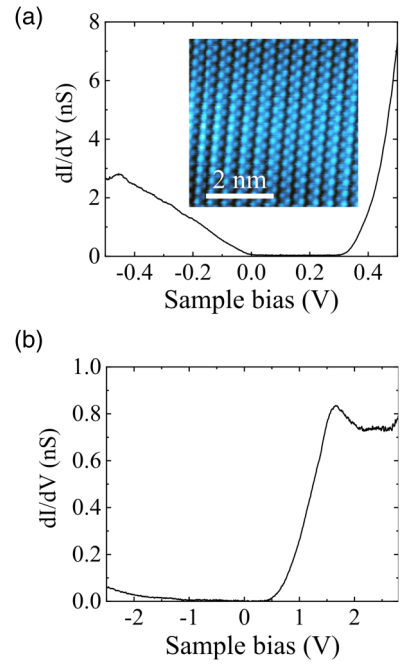

FIG. 4. (a) Experimental dI/dV spectrum of a bulk BP sample. The inset shows an STM image with atomic resolution of the area where the spectrum was measured (sample bias 0.2 V, tunneling current setpoint 600 pA), and (b) dI/dV spectrum measured over a larger sample bias range.

molecular orbital (LUMO) state is broader than the highest occupied molecular orbital (HOMO) state [14], which is distinctively different from what is observed on graphene [14,15]. This can be understood in a simple picture as a consequence of the asymmetric spatial extension of the B and AB states of BP. In a simple general picture, the broadening of a discrete level with an electron bath having a constant DOS, ρ, can be estimated to be $2\pi|\tau|^2\rho$, where τ is the coupling constants related to the overlap of the molecule and substrate wave functions. In the case of BP, the DOS is rather symmetric on both sides of the gap, while the vacuum LDOS is strongly asymmetric, as was reported above, resulting in asymmetric couplings τ. Therefore we argue that the asymmetric broadening of molecular states for molecules on BP is a consequence of different coupling strengths at positive and negative voltages but not of a different DOS of the substrate.

IV. CONCLUSIONS

We suggest that, quite generally, the bonding (B) or antibonding (AB) character of electronic states of a substrate can be very important for STM measurements. In particular, the B states have much less extension outside the substrate than the AB states, which should reflect in strong asymmetry of the STM spectra. We demonstrate this point on the BP, where both VB and CB are formed by p_z orbitals but have different character—bonding for VB and antibonding for CB. This will result in the much stronger conductance measured by STM at positive voltage compared to the negative one, which is in agreement with experimental observation. Moreover, that can also explain the asymmetric broadenings of frontier molecular orbitals (HOMO and LUMO) often observed for different molecules on BP.

ACKNOWLEDGMENTS

We are grateful to the ANR and MOST (DEFINE2D Project No. ANR-20-CE09-0023, MOST No. 110-2923-M-002 -010) for financial support. DFT calculations have been performed using HPC computation resources from TGCC-GENCI (Grant No. A0100910407).

[1] S. Tanaka, E. Ueda, M. Sato, K. Tamasaku, and S.-i. Uchida, Physica C **263**, 245 (1996).
[2] D. Li, C. Barreteau, S. L. Kawahara, J. Lagoute, C. Chacon, Y. Girard, S. Rousset, V. Repain, and A. Smogunov, Phys. Rev. B **93**, 085425 (2016).
[3] R. K. Tiwari, D. M. Otálvaro, C. Joachim, and M. Saeys, Surf. Sci. **603**, 3286 (2009).
[4] A. Chaika, S. Nazin, V. Semenov, S. Bozhko, O. Lübben, S. Krasnikov, K. Radican, and I. Shvets, EPL (Europhys. Lett.) **92**, 46003 (2010).
[5] A. Chaika, JETP Lett. **99**, 731 (2014).
[6] J. Riffle, C. Flynn, B. St. Laurent, C. Ayotte, C. Caputo, and S. Hollen, J. Appl. Phys. **123**, 044301 (2018).
[7] B. Kiraly, N. Hauptmann, A. N. Rudenko, M. I. Katsnelson, and A. A. Khajetoorians, Nano Lett. **17**, 3607 (2017).
[8] C. Zhang, J. Lian, W. Yi, Y. Jiang, L. Liu, H. Hu, W. Xiao, S. Du, L. Sun, and H. Gao, J. Phys. Chem. C **113**, 18823 (2009).
[9] X. Ling, H. Wang, S. Huang, F. Xia, and M. S. Dresselhaus, Proc. Natl. Acad. Sci. **112**, 4523 (2015).
[10] H. Guo, X. Cui, W. Zhou, D. Han, C. Lin, L. Cao, and M. Feng, J. Appl. Phys. **124**, 045301 (2018).
[11] P. Giannozzi, S. Baroni, N. Bonini, M. Calandra, R. Car, C. Cavazzoni, D. Ceresoli, G. L. Chiarotti, M. Cococcioni, I. Dabo *et al.*, J. Phys.: Condens. Matter **21**, 395502 (2009).
[12] P. Giannozzi, O. Andreussi, T. Brumme, O. Bunau, M. B. Nardelli, M. Calandra, R. Car, C. Cavazzoni, D. Ceresoli, M. Cococcioni *et al.*, J. Phys.: Condens. Matter **29**, 465901 (2017).
[13] Z. Qiu, H. Fang, A. Carvalho, A. Rodin, Y. Liu, S. J. Tan, M. Telychko, P. Lv, J. Su, Y. Wang *et al.*, Nano Lett. **17**, 6935 (2017).
[14] M. Bouatou, R. Harsh, C. Chacon, Y. Girard, V. Repain, A. Bellec, S. Rousset, A. Smogunov, Y. J. Dappe, and J. Lagoute, Adv. Mater. Interfaces **8**, 2101644 (2021).
[15] M. Bouatou, R. Harsh, F. Joucken, C. Chacon, V. Repain, A. Bellec, Y. Girard, S. Rousset, R. Sporken, F. Gao *et al.*, J. Phys. Chem. Lett. **11**, 9329 (2020).